The impact of hydrogen on the ductility loss of bainitic Fe–C alloys

T. Depover*, E. Van den Eeckhout and K. Verbeken

The influence of hydrogen on the mechanical properties of generic lab-cast Fe–C bainitic alloys is studied by tensile tests on notched samples. The bainitic microstructure is induced in a 0.2% C and 0.4% C Fe–C alloy by an appropriate heat treatment. The hydrogen embrittlement susceptibility is evaluated by mechanical tests on both *in situ* hydrogen pre-charged and uncharged specimens. The observed ductility loss of the materials is correlated with the present amount of hydrogen and the hydrogen diffusion coefficient. In addition to the correlation between the amount of hydrogen and the hydrogen-induced ductility loss, the hydrogen diffusion during the tensile test, quantified by the hydrogen diffusion distance during the test, appears to be of major importance as well.

Keywords: Hydrogen embrittlement, Mechanical properties, Fe–C alloys, Bainite, Diffusible hydrogen, Hydrogen diffusion coefficient

Introduction

The presence of hydrogen in steels is known to be detrimental for the overall use and more specific for the mechanical performance of the material. Moreover, the high susceptibility to hydrogen embrittlement (HE) appears to be an important issue in the development of advanced high strength steels.[1] Additionally, unpredicted hydrogen-induced failure may occur as well due to the increased tendency for cracking.[2,3] Although Johnson[4] discussed it for the first time in 1875, no full understanding of the mechanisms behind the HE phenomenon has been obtained so far. Therefore, proper insight on the interaction on a microstructural level between hydrogen and the investigated material is of great interest. Findley *et al*.[5] recently studied the mechanisms of hydrogen-induced cracking (HIC) in pipeline steels and reported that correlating hydrogen transport with cracking processes during HIC will enable to optimise alloy and microstructure design. The harmful impact of hydrogen on the mechanical performance of materials has already been thoroughly studied in numerous reference works by Bernstein,[6] Oriani[7] and Troiano.[8] Still, the responsible mechanisms remain under discussion and are subject of a lot of recent scientific work.

The HE phenomenon plays for instance an obstructing role for the material development in the automotive industry, where the aim is to reduce the vehicle's weight while retaining the same strength level to comply with safety regulations. High strength steels offer the desired properties. However, these steels are known to be more prone to HE.[9,10] Consequently, to comprehend or even predict the potential hydrogen-induced damage, further in-depth research on the interaction between hydrogen and high strength steels is required.

Department of Materials Science and Engineering, Ghent University (UGent), Technologiepark 903, B-9052 Ghent, Belgium

*Corresponding author, email tom.depover@ugent.be

This interaction has been evaluated by the present authors for four commercial steels[10–12] and an in-depth look was given to the transformation-induced plasticity (TRIP) material.[13] Unfortunately, thermal desorption spectroscopy (TDS) results indicated similar activation energies for the industrial steels and all the present peaks were at low temperature indicating the challenge of linking these peaks to a specific microstructural constituent.[12] Another work focused on the HE susceptibility for these commercial steels.[10] Generally, the hydrogen-induced mechanical degradation was more significant when the tensile test crosshead deformation speed was decreased demonstrating the importance of the hydrogen diffusion.

Alternatively, this specific hydrogen diffusion/material interaction has also been investigated in the work of Duprez *et al*.,[14] where emphasis was put on the impact of diffusible hydrogen on the hydrogen-induced ductility loss of high strength steels. The ductility loss after charging was reversible, since tensile tests performed on samples that were allowed to discharge in air for 1 week indicated that a large part of the ductility was recovered after discharging. Recently, Koyama *et al*.[15] studied the HIC behaviour for dual phase steels. They showed that both the hydrogen-enhanced decohesion and hydrogen-enhanced localised plasticity mechanisms contributed to the damage evolution. Additionally, Laureys *et al*.[16,17] studied the crack formation for TRIP steel and revealed that crack initiation started in the martensitic phase. However, the specific multiphase microstructure of these high strength steels is a complicating issue in correlating the effect of hydrogen with microstructural characteristics. Even in the detailed study on TRIP steel,[13] no conclusive interpretation of all TDS peaks to a certain microstructural constituent was possible. Therefore, in the present work, simplified lab-cast Fe–C alloys were submitted to an appropriate thermal treatment to induce a specific microstructural constituent, which remained somehow less investigated so far in literature, namely bainite.

Received 2 November 2015; accepted 28 December 2015
DOI 10.1080/02670836.2015.1137387

The HE susceptibility of different steel microstructures has been described by many authors in literature. Chan[18] presented an overview and showed that an as-quenched martensitic structure appears to be most prone to HE. Additionally, the as-quenched martensite contains the lowest hydrogen diffusivity due to the dense microstructure.[19–21] On the contrary, tempered bainite or martensite has the best resistance against the hydrogen-induced ductility loss, while the pearlitic structure performs in between.[22] In another study on the hydrogen diffusivity of different microstructural features, Chan and Charles[23] found that martensite demonstrated the highest hydrogen solubility together with the lowest hydrogen diffusivity. Furthermore, the hydrogen diffusivity was higher for upper and lower bainite compared to the ferrite/pearlite microstructure. Moreover, Chan[18] also investigated the effect of the carbon content on the hydrogen-trapping capacity in ferrite–pearlite steels. They showed that the hydrogen saturation level increased with carbon content until the carbon content of 0.69% (i.e. near the eutectoid composition), which was correlated with the importance of the pearlite/ferrite interface.[24] A martensitic phase with variable carbon content was studied as well in Chan *et al.*,[25] where the martensite morphology was correlated with the present amount of hydrogen.

The susceptibility to the hydrogen-induced ductility loss has been reported to be less for bainitic steels compared to other microstructural phases for certain environments causing HE and corrosion fatigue.[26–29] The mechanical degradation was analysed by performing slow strain rate tensile tests in Kerns *et al.*,[26] Fujita and Yamada[27] and Bernstein and Thompson[28] and it was observed that lower bainite showed the highest resistance against HE when compared to quenched and tempered martensite, normalised ferrite/pearlite, spheroidised microstructures and untempered martensite.

Luppo and Ovejero-Garcia[30] correlated the HE sensitivity with the hydrogen diffusivity and desorption kinetics in a low carbon steel in which several microstructures are induced by an appropriate heat treatment. They found that the desorption kinetics were minimum for an as-quenched martensitic structure, whereas the amount of desorbed hydrogen was maximal. Moreover, they saw that the HE susceptibility could be correlated with the amount of desorbed hydrogen. This meant that diffusible hydrogen could be set responsible for the hydrogen-induced ductility loss, which is in good correspondence to already published results.[10,14,31–33]

Tau *et al.*[34] studied three different tempered martensitic and bainitic structures and observed that the carbides' characteristics influenced the hydrogen diffusivity. Moreover, the carbides in bainite may even play a determinant factor in retarding the hydrogen transport, which explained why samples with very fine carbides showed the highest amount of hydrogen. The specific interaction between the hydrogen-trapping capacity and carbide-forming elements has been evaluated as well before.[35–40]

In this study, the complex microstructure of industrial steels was avoided by focusing on a specific microstructural component which was induced in lab-cast generic Fe–C alloys by a well-designed thermal cycle. Two bainitic microstructures, induced in alloys with variable carbon content, were evaluated for their interaction with hydrogen. The impact of hydrogen charging on the mechanical properties was evaluated by comparing tensile tests on *in situ* hydrogen-charged samples with those performed on uncharged specimens. Apart from the effect of carbon, tensile tests performed at variable crosshead deformation speed allowed visualising the role of hydrogen diffusion in the mechanical degradation. As such a straightforward interpretation on the role of the amount of hydrogen and hydrogen diffusivity in hydrogen-induced degradation in a bainitic microstructure could be obtained.

Experimental procedure

Material characterisation

The lab-cast alloys were two Fe–C materials containing 0.2% and 0.4% of carbon, respectively. The chemical compositions are given in Table 1.

The alloys were produced in a Pfeiffer VSG100 vacuum melting and casting unit, operating under an argon gas protective atmosphere. The materials were hot rolled till 8 mm and then cold rolled to a final thickness of 1.6 mm. An appropriate heat treatment was applied on the Fe–C grades to induce a bainitic microstructure, as presented in Fig. 1. In a first stage, both grades were heated to 900°C in a salt bath for 10 minutes and immediately transferred to a second salt bath, where they were hold at 400°C for 10 minutes. The grade was then air cooled.

All samples were then ground and tensile samples were machined with their tensile axis parallel to the rolling direction. Finally, the surface and edges of the sample were sandblasted to remove possible remaining oxides. After sandblasting another 0.1 mm of material was removed till a final thickness of 1.5 mm was reached. For light optical microscopy (LOM), sample surfaces were ground, polished and finally etched with 2% Nital for 10 seconds. The phase content of each lab-cast material was determined by an image analysis program (Image J®). This is important to be able to evaluate the impact of the introduced phases on the HE resistance. An average of five images gave an approximate value of each phase.

Mechanical characterisation

The HE impact on the mechanical behaviour was evaluated by comparing tensile tests in air with tests performed on hydrogen-charged samples. Two tests performed under the same conditions will be labelled as 'A' and 'B'.

Table 1 Chemical composition of the used materials in wt-%

Material/element	C	Mn	Si	Other
0.2% C	0.199	0.004	<0.0002	<0.0008 P, N
0.4% C	0.374	0.002	<0.0001	<0.0007 P, N

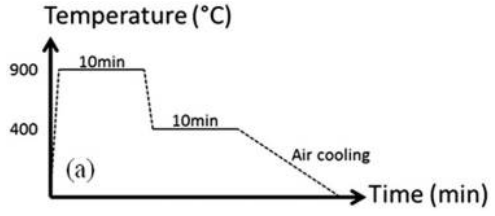

1 Temperature–time graph of the used heat treatment to generate bainite

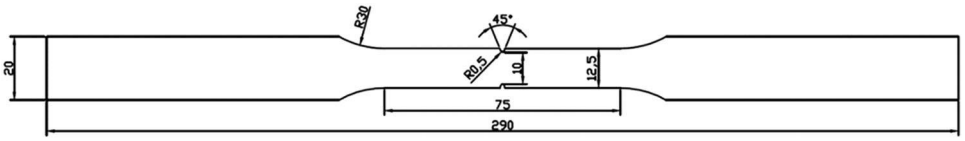

2 Geometry of the tensile specimen

Hydrogen was introduced by cathodic charging using 1 g L^{-1} of thiourea in a 0.5 M H_2SO_4 solution. The materials were pre-charged for 2 hours at a current density of 2.65 mA cm^{-2}, while *in situ* charging continued during the actual tensile test. Moreover, these charging conditions were chosen in such a way that they did not create hydrogen blisters or internal damage in the sample and that complete hydrogen saturation was ensured.[41] Notched tensile samples (Fig. 2), which due to the notch locally introduce a triaxial stress state, were used to control crack initiation. This geometrical discontinuity leads to a local stress concentration, which is expressed by a stress concentration factor K_t of 4.2.

Tensile tests were performed using two different crosshead deformation speeds; namely 5 mm min^{-1}, similar to Zhao *et al.*,[42] and 0.05 mm min^{-1}, with a corresponding strain rate of 1.11×10^{-3} and 1.11×10^{-5} s^{-1}. This variation in crosshead deformation speed allowed evaluating the possible effect of hydrogen diffusion during the actual test. An embrittlement index (EI) is established in order to evaluate the impact of hydrogen on the ductility of the different materials and defined as:

$$\mathrm{EI} = \frac{\text{Elongation in Air} - \text{Elongation when Charged}}{\text{Elongation in Air}} \tag{1}$$

Hence, the EI varies between 0 and 1, with 0 meaning that there is no ductility loss and the material is insensitive to HE. When an index of 1 is obtained, the ductility drop is 100% and HE is maximal.

Determination of diffusible and total hydrogen content

To determine the hydrogen content, samples were charged electrochemically using the same conditions as while *in situ* charging. In order to determine the hydrogen saturation level, melt/hot extraction was used. Measurements were done at 1600°C for the total hydrogen and at 300°C for the diffusible hydrogen content, which is the same definition for diffusible hydrogen as proposed by Wang *et al.*[43] and Akiyama *et al.*[44]

Determination of hydrogen diffusion coefficient

To determine the hydrogen diffusion coefficient, hydrogen electrochemical permeation tests were performed according to the Devanathan and Stachurski method.[45] The two compartments were filled with 0.1 M NaOH solution and the polished specimen of 1 mm thickness was clamped in between. The hydrogen entry side acted as the cathode by applying a current density of 3 mA cm^{-2}, and the hydrogen exit side (anode) was potentiostatically kept at −500 mV with respect to a Hg/Hg_2SO_4 reference electrode. This electrolyte differs from the one used for the tensile tests as the high current density and long duration of the permeation test are very likely to cause hydrogen-induced damage such as blisters which would make the obtained results unvalid.[11] The solutions in the compartments were both stirred with nitrogen bubbling and temperature was maintained constant at 25°C. The apparent hydrogen diffusion coefficient was calculated from the permeation transient using the following formula[46]:

$$D_{\mathrm{app}} = \frac{L^2}{7.7t} \left(\mathrm{m^2\ s^{-1}}\right) \tag{2}$$

where t is the time when the normalised steady-state value has reached 0.1 and L is the specimen thickness.

Material characterisation

Figure 3 presents the LOM images of the material with 0.2% C and 0.4% C in which a bainitic structure is induced, respectively referred to as B2 and B4. Rolling and normal directions are shown in the image. Additionally, the phase content was calculated using the above-mentioned procedure to obtain an indication of the amount of bainite, as shown in Table 2.

The desired microstructural constituents are clearly present in Fig. 3. B4 clearly contained a higher fraction of the desired constituent being a nearly 100% bainitic material. A noticeable feature is present in the B2 microstructure (Fig. 3*a*), which could be identified as Widmanstätten ferrite (α_w). This microstructural feature is produced in the higher temperature region of the bainitic transformation region.[31,47] The mechanism to form Widmanstätten ferrite is displacive (strain-dominated) and reconstructive (diffusion-dominated). The faster moving interstitial atoms diffuse and spread between the phases. This is exactly how Widmanstätten ferrite grows: a displacive mechanism whose rate is controlled by the diffusion of carbon in the austenite ahead of the α_w/g interface.[47] B4 does not contain Widmanstätten ferrite. The bainitic transformation curves in a temperature–time transformation diagram move to the right when the carbon content increases, meaning that more time becomes available to cool the material till the desired temperature for bainite formation, which is 400°C in the present case. Since the same heat treatment was applied for both grades, the Widmanstätten ferrite zone got intersected in the case of B2, resulting in some ferrite in the microstructure in contrast to B4 which had a nearly homogeneous bainitic structure.

Table 2 Average phase content determined based on the average of five micrographs

	Phase content (%)
B2	89.2% bainite + 10.8% ferrite
B4	98.1% bainite + 1.9% ferrite

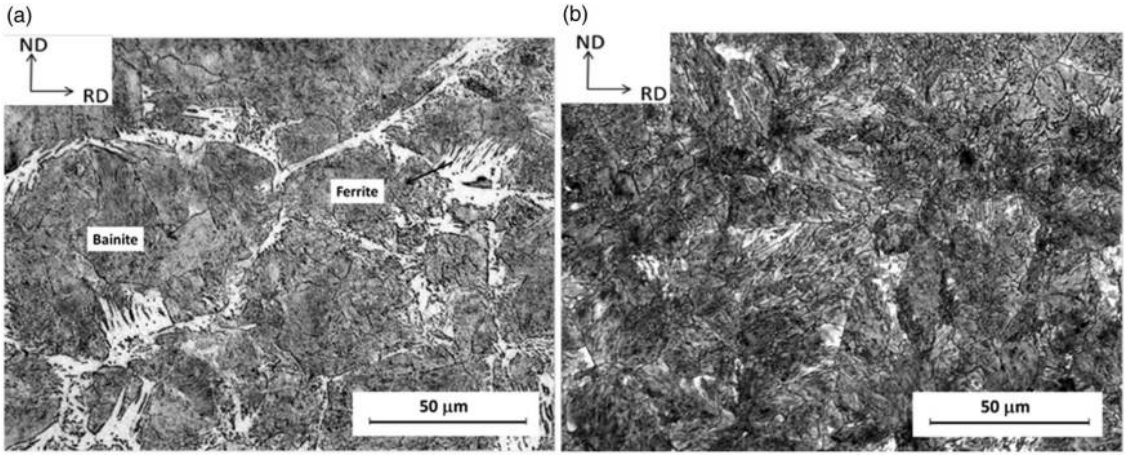

3 Optical microstructures of the Fe–0.2% C bainitic (B2) *a* and Fe–0.4% C bainitic (B4) alloy *b*

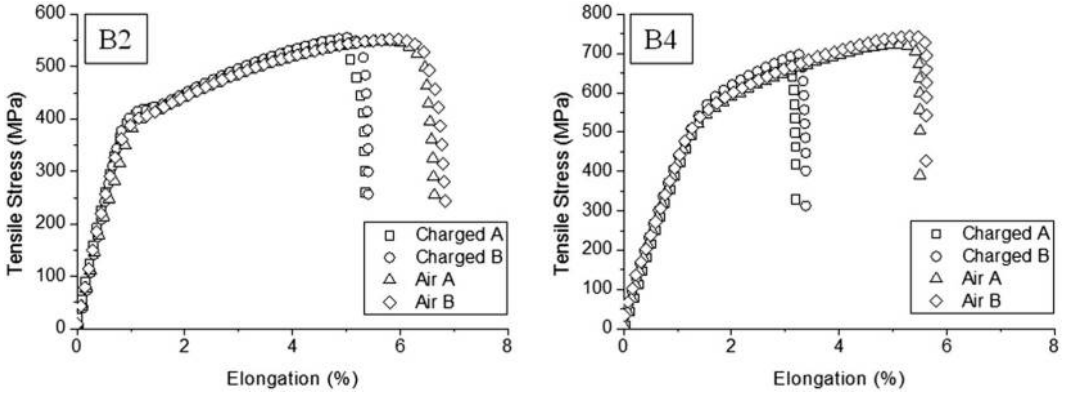

4 Stress–strain curves at crosshead deformation speed of 5 mm min^{-1} for B2 and B4, with similar tests indicated with 'A' and 'B'

Tensile tests at 5 mm min^{-1}

Figure 4 shows the results of the tensile tests performed on the different materials at a crosshead deformation speed of 5 mm min^{-1} in uncharged condition (air) and after hydrogen charging. The reproducibility of the different tests was very good and the results are summarised in Table 3.

B4 had an increased strength level compared to B2 due to the higher carbon content and the higher amount of bainite: B4 (98% B) compared to B2 (89% B). Additionally, the hydrogen-induced ductility loss is larger for B4 compared to B2, which is in good agreement with the correlation between HE sensitivity and the strength level of the material.[9,10] In addition, the effect of the presence of hydrogen was elaborated as well as discussed in the next section by determining the hydrogen content in both alloys.

Determination of the hydrogen uptake capacity

The hydrogen uptake capacity was studied based on melt/hot extraction results. With respect to the hydrogen uptake capacity, it is important to make a distinction between the amount of diffusible hydrogen, released from the sample by heating to 300°C, and the total amount of hydrogen, released from the sample by melting, since the diffusible hydrogen has been argued to play a crucial role in HIC.[30,33] The results are presented in Table 4.

The total and diffusible hydrogen content is higher for B4. This could be correlated with the higher amount of bainite in B4 compared to B2. An almost fully bainitic microstructure was obtained for B4, while some Widmanstätten ferrite was present in B2, as shown in Fig. 3. Also the higher carbon content for B4 explains this observed tendency since generally the hydrogen uptake capacity increases with carbon content.[18,31,41] Additionally, Hadam and Zakroczymski[48] studied the absorption of

Table 3 Summary of the tensile tests performed at a crosshead deformation speed of 5 mm min^{-1}

	Tensile strength/MPa	El/%
B2	550	21
B4	733	40

Table 4 Melt (1600°C) and hot (300°C) extraction results for hydrogen saturated samples in wppm

	Total hydrogen/wppm	Diffusible hydrogen/wppm
B2	8.71 ± 0.54	3.82 ± 0.12
B4	14.65 ± 0.74	8.73 ± 0.52

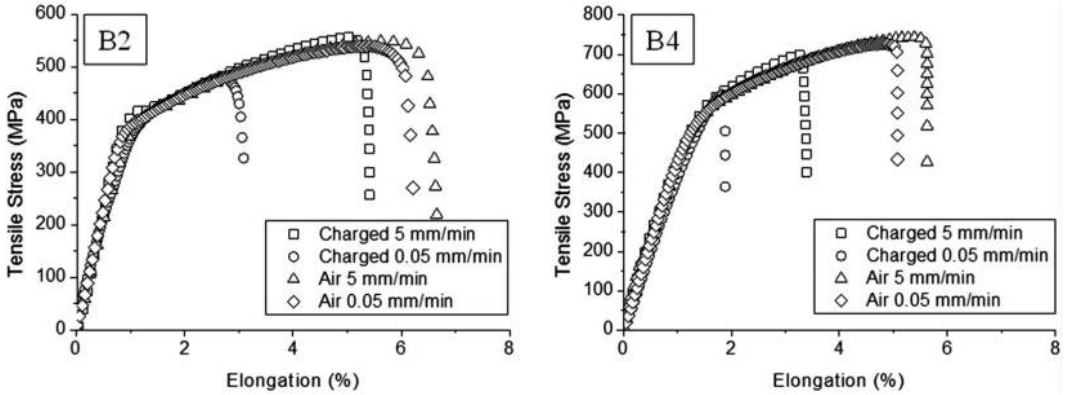

5 Stress–strain curves for B2 and B4 at crosshead deformation speed of 5 and 0.05 mm min^{-1}

hydrogen in relation to the carbon content in gradually strained Armco iron (0.05% C) and high carbon steel (1.00% C) using electrochemical permeation and TDS. They also found a considerable higher amount of hydrogen in the high carbon alloy.

The higher EI for B4 (40%) compared to B2 (21%) is in correspondence with the higher amount of diffusible hydrogen introduced by electrochemical charging, i.e. 8.73 and 3.82 wppm, respectively. This correlation between EI and amount of diffusible hydrogen has been confirmed in literature,[30–33] but as we have previously shown the hydrogen diffusion coefficient should also be incorporated in this discussion.[10,14,31] Therefore, the hydrogen diffusion distance in the microstructure at a specific crosshead deformation speed, i.e. during the course of the tensile test, should also be linked with the observed EIs. When a crosshead deformation speed of 5 mm min^{-1} is applied, the test duration always remained below 1 minute in the present material. In order to have a more outspoken effect of hydrogen diffusion and to obtain an experimental validation for the proposed importance of the combined impact of both the amount of diffusible hydrogen and the hydrogen diffusivity, tensile tests were performed at a crosshead deformation speed which is 100 times slower.

Tensile tests at 0.05 mm min^{-1}

Tensile samples were tested at a significantly lower crosshead deformation speed of 0.05 mm min^{-1}. Hence, diffusible hydrogen had more time to diffuse to the crack tip and play its detrimental role. The influence of the deformation rate was already mentioned by Toh and Baldwin,[49] who demonstrated that the reduction of area decreased with increasing deformation rate, and by the present authors for some advanced high strength steels.[10,50] Each test was performed twice to guarantee reproducible results. The results are summarised in Fig. 5, where for the sake of clarity only one of two performed tests is shown.

Generally, the degree of embrittlement increased with lower crosshead deformation speed, which is in good agreement to what has been observed in literature.[10,31,50] Although B4 showed the lowest absolute elongation, the increased HE sensitivity was clearly more pronounced for B2 (from 21 to 50%) compared to B4 (from 40 to 63%). Nevertheless, the amount of diffusible hydrogen was higher for B4 (cf. Table 4). Since *in situ* hydrogen charging was applied and due to the longer test times at 0.05 mm min^{-1}, the effect of hydrogen diffusion is believed to play a more crucial role for these lower crosshead deformation speed tests. Therefore, an in-depth analysis of the hydrogen diffusivity is elaborated in the next section.

Determination of the hydrogen diffusion coefficient

An indication of the distance x (cm) hydrogen can diffuse during the tensile test can be calculated by taking the square root of the product of the diffusion coefficient D (cm^2 s^{-1}) and the duration time t (seconds) of the tensile test, i.e. $x = (D \times t)^{1/2}$, as was also done by Koyama *et al.*[15] Consequently, the actual hydrogen diffusion distance can be determined and correlated with the observed hydrogen-induced ductility loss. Hydrogen permeation tests were performed and the results are presented in Fig. 6. The calculated diffusion coefficients, determined as described in Section 'Experimental procedure', are summarised in Table 5.

The hydrogen diffusion coefficient is significantly lower for B4 due to the higher amount of bainite compared to

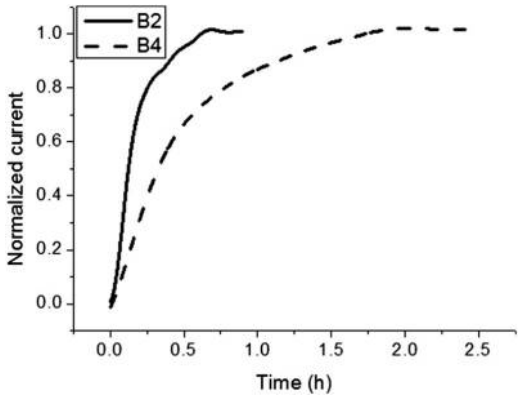

6 Hydrogen permeation curves for B2 and B4

Table 5 Hydrogen diffusion coefficient for B2 and B4

	Hydrogen diffusion coefficient
B2	6.71×10^{-10} m^2 s^{-1}
B4	3.40×10^{-10} m^2 s^{-1}

Table 6 The embrittlement indices at 5 and 0.05 mm min^{-1} together with the amount of diffusible hydrogen and the distance *x* hydrogen can diffuse during a tensile test at 5 and 0.05 mm min^{-1}

	EI at 5 mm min^{-1}/%	EI at 0.05 mm min^{-1}/%	Diffusible H/wppm	*x* at 5 mm min^{-1}/ mm	*x* at 0.05 mm min^{-1}/mm
B2	21	50	3.82	0.18	1.36
B4	40	63	8.73	0.10	0.76

B2 and the higher amount of carbon which impedes hydrogen diffusion, which is in correspondence with the work of Hadam and Zakroczymski,[48] who also mentioned that the lattice diffusivity of hydrogen in the low carbon alloy was higher than in the high carbon steel. When these curves are compared to the ideal Fick's law, the transient is less steep and more extended. This is attributed to the presence of hydrogen-trapping sites which delay the experimental transient compared to the theoretical curve described by Fick's law which assumes ideal diffusion. The embrittlement indices together with the amount of diffusible hydrogen and the approximate distance *x* over which hydrogen can diffuse during the tensile test are summarised in Table 6.

The combined effect of the amount of diffusible hydrogen and the hydrogen diffusivity is clearly demonstrated when comparing B2 and B4 at a crosshead deformation speed of 0.05 mm min^{-1}. Indeed, the effect of lowering the crosshead deformation speed was more pronounced in B2 (EI from 21 to 50%) compared to B4 (EI from 40 to 63%), even though the amount of diffusible hydrogen was higher for B4. This observation is a consequence of the larger distance *x* that the diffusible hydrogen can migrate during the test in B2. Diffusible hydrogen is expected to play a major role in HE because of its interactions with dislocations, its role during crack initiation and propagation. Additionally, hydrogen is attracted to highly stressed zones ahead of the crack tip. The ability to more easily reach these critical stress zones assists crack propagation at lower crosshead deformation speed, which results in an increase of the hydrogen-induced ductility loss. The lower diffusion coefficient in B4 explains the lower increase in EI for this material when lowering the tensile test speed. Alternatively, at the higher crosshead deformation speed, only a limited diffusion could take place and therefore in this material the amount of diffusible hydrogen plays a more prominent role in the observed EI for the different materials.

Conclusion

Tensile tests combined with *in situ* hydrogen charging were performed on generic lab-cast Fe–C alloys. A bainitic microstructure was induced in a 0.2% C (B2) and 0.4% C (B4) Fe–C alloy by an appropriate heat treatment. While the B2 alloy contained about 89% bainite, about 98% of bainite was present in the B4 alloy. The tensile tests demonstrated a considerable ductility loss due to hydrogen pick-up, although the degree of embrittlement varied considerably between the grades. Increasing the carbon content up to 0.4% for the bainitic microstructure resulted in an increased HE due to the larger amount of diffusible hydrogen, 3.82 and 8.73 wppm hydrogen for B2 and B4, respectively. The influence of the hydrogen diffusion coefficient was negligible for a crosshead deformation speed of 5 mm min^{-1}.

Tensile tests performed at a lower crosshead deformation speed of 0.05 mm min^{-1} allowed to further elaborate the combined effect of both the amount of diffusible hydrogen and the hydrogen diffusion during the test. An additional ductility loss was observed. It was clearly demonstrated that, although adding carbon resulted in a higher amount of diffusible hydrogen, a lower increase in terms of HE was obtained for B4 (EI from 40 to 61%) compared to B2 (EI from 21 to 48%) when lowering the crosshead deformation speed. This was related to the lower hydrogen diffusion coefficient of B4. This nicely confirmed the reasoning that a direct link between the measured amount of diffusible hydrogen and the increased embrittling behaviour when lowering the tensile test speed is impossible without also incorporating the hydrogen diffusion coefficient of that specific microstructure into the discussion.

Acknowledgements

The authors wish to thank the Special Research Fund (BOF), UGent (BOF10/ZAP/121) and the Agency for Innovation by Science and Technology in Flanders (IWT) for support (Project nr SB111205). The authors also acknowledge the technicians and staff working at the hydrogen laboratory at ArcelorMittal R&D Gent and the technical staff from the Department of Materials Science and Engineering, UGent, for their help with the experiments and sample preparation.

References

1. M. Loidl and O. Kolk: 'Hydrogen embrittlement in HSSs limits use in lightweight body', *Adv. Mater. Process.*, 2011, **169**, (3), 22–25.
2. H. K. D. H. Bhadeshia and W. Solano-Alvarez: 'Critical assessment 13: elimination of white etching matter in bearing steels', *Mater. Sci. Technol.*, 2015, **31**, (9), 1011–1015.
3. J. Woodtli and R. Kieselbach: 'Damage due to hydrogen embrittlement and stress corrosion cracking', *Eng. Fail. Anal.*, 2000, **7**, 427–450.
4. W. H. Johnson: 'On some remarkable changes produced in iron and steel by the action of hydrogen and acids', *Proc. R. Soc. London*, 1874, **23**, 168–179.
5. K. O. Findley, M. K. O'Brien and N. Nako: 'Critical assessment: mechanisms of hydrogen induced cracking in pipeline steels', *Mater. Sci. Technol.*, 2015, **31**, 1673–1680.
6. I. M. Bernstein: 'The role of hydrogen in the embrittlement of iron and steel', *Mater. Sci. Eng.*, 1970, **6**, 1–19.
7. R. A. Oriani: 'Hydrogen embrittlement of steels', *Ann. Rev. Mater. Sci.*, 1978, **8**, 327–357.
8. A. R. Troiano: 'Hydrogen embrittlement of high strength FCC alloys', in '*Hydrogen in metals*', (ed. I. M. Bernstein and A. W. Thomson), 3–16; 1974, Metals Park, OH, ASM.
9. T. B. Hilditch, S.-B. Lee, J. G. Speer and D. K. Matlock: 'Response to hydrogen charging in high strength automotive sheet steel products', *SAE Technical Paper*, 2003, DOI 10.4271/2003-01-0525.
10. T. Depover, D. Pérez Escobar, E. Wallaert, Z. Zermout and K. Verbeken: 'Effect of hydrogen charging on the mechanical properties of advanced high strength steels', *Int. J. Hydrogen Energ.*, 2014, **39**, 4647–4656.
11. D. Pérez Escobar, T. Depover, E. Wallaert, L. Duprez, M. Verhaege and K. Verbeken: 'Thermal desorption spectroscopy study of the interaction between hydrogen and different microstructural constituents in lab cast Fe–C alloys', *Corros. Sci.*, 2012, **65**, 199–208.
12. D. Pérez Escobar, K. Verbeken, L. Duprez and M. Verhaege: 'Evaluation of hydrogen trapping in high strength steels by thermal

desorption spectroscopy', *Mat. Sci. Eng. A-Struct.*, 2012, **551**, 50–58.
13. D. Pérez Escobar, T. Depover, L. Duprez, K. Verbeken and M. Verhaege: 'Combined thermal desorption spectroscopy, differential scanning calorimetry, scanning electron microscopy and X-ray diffraction study of hydrogen trapping in cold deformed TRIP steel', *Acta Mater.*, 2012, **60**, 2593–2605.
14. L. Duprez, K. Verbeken and M. Verhaege: 'Effect of hydrogen on the mechanical properties of multiphase high strength steels', in '*Effect of hydrogen on materials*', (ed. B. P. Somerday et al.), 62–69; 2008, Wyoming, USA, ASM International.
15. M. Koyama, C. C. Tasan, E. Akiyama, K. Tsuzaki and D. Raabe: 'Hydrogen-assisted decohesion and localized plasticity in dual-phase steel', *Acta Mater.*, 2014, **70**, 174–187.
16. A. Laureys, T. Depover, R. Petrov and K. Verbeken: 'Characterization of hydrogen induced cracking in TRIP-assisted steels', *Int. J. Hydrogen Energ.*, 2015, **40**, 16901–16912.
17. A. Laureys, T. Depover, R. Petrov and K. Verbeken: 'Microstructural characterization of hydrogen induced cracking in TRIP-assisted steel by EBSD', *Mater. Charact.*, 2016, **112**, 169–179.
18. S. L. I. Chan: 'Hydrogen trapping ability of steels with different microstructures', *J. Chin. Inst. Eng.*, 1999, **22**, 43–53.
19. E. Snape: 'Roles of composition and microstructure in sulfide cracking of steel', *Corrosion*, 1968, **24**, 261–282.
20. R. M. Hudson and G. L. Stragand: 'Effect of cold drawing on hydrogen behavior in steel', *Corrosion*, 1960, **16**, 253t–258t.
21. B. Marandet: 'Effect of cold work on the dissolution and the diffusion of hydrogen in unalloyed carbon steels', Proc. Int. Conf. on 'Stress corrosion cracking and hydrogen embrittlement of iron base alloys', Houston, USA, 1977, NACE, 774–787.
22. A. W. Thompson and I. M. Bernstein: 'The role of metallurgical variables in hydrogen-assisted environmental fracture', in '*Advances in corrosion science and technology*' (ed. M. G. Fontana and R. W. Staehle), Vol. 7, 53–175; 1980, New York, Plenum Press.
23. S. L. I. Chan and J. A. Charles: 'Hydrogen occlusivity of steels with different microstructures', Proc. 5th Asian-Pacific corrosion control Conf., Vol. 2, Melbourne, Australia, 1987.
24. S. L. I. Chan and J. A. Charles: 'Effect of carbon content on hydrogen occlusivity and embrittlement of ferrite–pearlite steels', *Mater. Sci. Technol.*, 1986, **2**, 956–962.
25. S. L. I. Chan, H. L. Lee and J. R. Yang: 'Effect of carbon content and martensitic morphology on hydrogen occlusivity and effective hydrogen diffusivity', Proc. 4th Int. Conf. on 'The effect of hydrogen on the behavior of materials', PA, 1990, 145–155 .
26. G. E. Kerns, M. T. Wang and R. W. Staehle: 'Stress corrosion cracking and hydrogen embrittlement in high strength steels', in '*Stress corrosion cracking and hydrogen embrittlement of iron base alloys*', (ed. R. W. Staehle et al.), 700; 1977, Houston, TX, NACE-5.
27. T. Fujita and Y. Yamada: 'Physical metallurgy and SCC in high strength steels', in '*Stress corrosion cracking and hydrogen embrittlement of iron base alloys*', (ed. R. W. Staehle et al.), 736; 1977, Houston, TX, NACE-5.
28. I. M. Bernstein, A. W. Thompson: 'Hydrogen in materials', in '*Advances in corrosion science and technology*', (ed. M. G. Fontana and R. W. Staehle), Vol. 7, 53; 1988, New York, Plenum Press.
29. F. C. Akbasoglu and D. V. Edmonds: 'Rolling contact fatigue and fatigue crack propagation in 1C–1.5Cr bearing steel in the bainitic condition', *Metall. Trans. A*, 1990, **21**, 889.
30. M. I. Luppo and J. Ovejero-Garcia: 'The influence of microstructure on the trapping and diffusion of hydrogen in a low carbon steel', *Corros. Sci.*, 1991, **32**, 1125–1136.
31. T. Depover, D. Pérez Escobar, E. Wallaert and K. Verbeken: unpublished work, 2015.
32. T. Depover, O. Monbaliu, E. Wallaert and K. Verbeken: 'Effect of Ti, Mo and Cr based precipitates on the hydrogen trapping and embrittlement of Fe–C–X Q&T alloys', *Int. J. Hydrogen Energ.*, 2015, **40**, 16977–16984.
33. P. Novak, R. Yuan, B. P. Somerday, P. Sofronis and R. O. Ritchie: 'A statistical physical-based, micro-mechanical model of hydrogen-induced intergranular fracture in steel', *J. Mech. Phys. Solids*, 2010, **58**, 206–226.
34. L. Tau, S. L. I. Chan and C. S. Shin: 'Hydrogen enhanced fatigue crack propagation of bainitic and tempered martensitic steels', *Corros. Sci.*, 1996, **38**, 2049–2060.
35. E. Wallaert, T. Depover, M. A. Arafin and K. Verbeken: 'Thermal desorption spectroscopy evaluation of the hydrogen-trapping capacity of NbC and NbN precipitates', *Metall. Mater. Trans. A*, 2014, **45**, 2412–2420.
36. T. Depover, E. Van den Eeckhout, E. Wallaert, Z. Zermout and K. Verbeken: 'Evaluation of the effect of TiC precipitates on the hydrogen trapping capacity of Fe–C–Ti alloys', *Advanced Materials Research*, 2014, **922**, 102–107.
37. D. Pérez Escobar, E. Wallaert, L. Duprez, A. Atrens and K. Verbeken: 'Thermal desorption spectroscopy study of the interaction of hydrogen with TiC precipitates', *Met. Mater. Int.*, 2013, **19**, 741–748.
38. F. G. Wei, T. Hara and K. Tsuzaki: 'Precise determination of the activation energy for desorption of hydrogen in two Ti-added steels by a single thermal-desorption spectrum', *Metall. Mater. Trans. B*, 2004, **35**, 587–597.
39. F. G. Wei and K. Tsuzaki: 'Quantitative analysis on hydrogen trapping of TiC particles in steel', *Metall. Mater. Trans. A*, 2006, **37**, 331–353.
40. J. Takahashi, K. Kawakami, Y. Kobayashi and T. Tarui: 'The first direct observation of hydrogen trapping sites in TiC precipitation-hardening steel through atom probe tomography', *Scripta Mater.*, 2010, **63**, 261–264.
41. D. Pérez Escobar, C. Miñambres, L. Duprez, K. Verbeken and M. Verhaege: 'Internal and surface damage of multiphase steels and pure iron after electrochemical hydrogen charging', *Corros. Sci.*, 2011, **53**, 3166–3176.
42. M.-C. Zhao, M. Liu, A. Atrens, Y.-Y. Shan and K. Yang: 'Effect of applied stress and microstructure on sulfide stress cracking resistance of pipeline steels subject to hydrogen sulfide', *Mat. Sci. Eng. A-Struct.*, 2008, **478**, 43–47.
43. M. Wang, E. Akiyama and K. Tsuzaki: 'Effect of hydrogen on the fracture behavior of high strength steel during slow strain rate test', *Corros. Sci.*, 2007, **49**, 4081–4097.
44. E. Akiyama, K. Matsukado, M. Wang and K. Tsuzaki: 'Evaluation of hydrogen entry into high strength steel under atmospheric corrosion', *Corros. Sci.*, 2010, **52**, 2758–2765.
45. M. A. V. Devanathan and Z. O. J. Stachurski: 'The adsorption and diffusion of electrolytic hydrogen in palladium', *Proceedings of the Royal Society A: Mathematical, Physical and Engineering Sciences*, 1962, **270**, 90.
46. J. McBreen, L. Nanis and W. Beck: 'A method for determination of the permeation rate of hydrogen through metal membranes', *J. Electrochem. Soc.*, 1966, **113**, 1218–1222.
47. H. K. D. H. Bhadeshia: 'Interpretation of the microstructure of steel', University of Cambridge, England; available at http://www.msm.cam.ac.uk/phase-trans/2000/C9/lecture7.pdf
48. U. Hadam and T. Zakroczymski: 'Absorption of hydrogen in tensile strained iron and high carbon steel studied by electrochemical permeation and desorption techniques', *Int. J. Hydrogen Energ.*, 2009, **34**, 2449–2459.
49. T. Toh and W. M. Baldwin: 'Ductility of steel with varying concentrations of hydrogen', in '*Stress corrosion cracking and embrittlement*', (ed. W. D. Robertson), 176–186; 1956, New York, Wiley.
50. T. Depover, E. Wallaert and K. Verbeken: 'Fractographic analysis of the role of hydrogen diffusion on the hydrogen embrittlement susceptibility of DP steel', *Mat. Sci. Eng. A-Struct.*, 2016, **649**, 201–208.